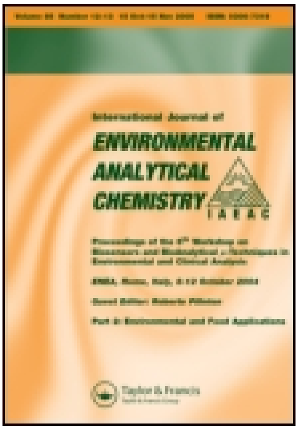

International Journal of Environmental Analytical Chemistry
Publication details, including instructions for authors and subscription information:
http://www.tandfonline.com/loi/geac20

Synthesis and applications of novel attapulgite-supported Co(II)-imprinted polymers for selective solid-phase extraction of cobalt(II) from aqueous solutions

Chunxiang Li [a], Jianming Pan [a], Xiaohua Zou [a], Jie Gao [a], Jimin Xie & Yan Yongsheng [a]

[a] School of Chemistry and Chemical Engineering, Jiangsu University, Zhenjiang 212013, China

To cite this article: Chunxiang Li, Jianming Pan, Xiaohua Zou, Jie Gao, Jimin Xie & Yan Yongsheng (2011): Synthesis and applications of novel attapulgite-supported Co(II)-imprinted polymers for selective solid-phase extraction of cobalt(II) from aqueous solutions, International Journal of Environmental Analytical Chemistry, 91:11, 1035-1049

To link to this article: http://dx.doi.org/10.1080/03067310903502752

Intern. J. Environ. Anal. Chem.
Vol. 91, No. 11, 15 September 2011, 1035–1049

Synthesis and applications of novel attapulgite-supported Co(II)-imprinted polymers for selective solid-phase extraction of cobalt(II) from aqueous solutions

Chunxiang Li, Jianming Pan, Xiaohua Zou, Jie Gao, Jimin Xie
and Yan Yongsheng*

School of Chemistry and Chemical Engineering, Jiangsu University, Zhenjiang 212013, China

(*Received 20 July 2009; final version received 18 November 2009*)

A simple and reliable approach using surface imprinting technique combined with chitosan incorporated sol-gel process was established to synthesise a novel Co(II)-imprinted polymer (Co-IIP) with attapulgite as the support material. Then the prepared polymer was characterised by using fourier tranmission infrared spectra (FT-IR) and scanning electron microscopy (SEM), and the imprinting mechanism of Co-IIP was proposed. Batch experiments studies were performed to evaluate the adsorption kinetics, selective recognition, adsorption isotherm, desorption and regeneration characters of Co-IIP. Results showed that Co-IIP offered fast kinetics for the adsorption and desortion Co^{2+} under the optimum conditions. The adsorption and selective recognition Co^{2+} were both followed the order Co-IIP > attapulgite > NIP. Moreover, Langmuir adsorption isotherm fitted well for the experimental equilibrium data of Co-IIP, and the maximum adsorption capacity of Co-IIP was $31.5\,mg\,g^{-1}$. Furthermore, Co-IIP could be reused four times with only about 13.42 ~ 16.17% regeneration loss, and the enrichment factor was more than 10.0. The developed method was also successfully applied to the determination of trace Co^{2+} in river sediments with satisfactory results. The relative standard deviation of the method (RSD) and the detection limit (3σ) were 1.35% and 0.0263, respectively.

Keywords: ion-imprinted; Co(II) ion; attapulgite; adsorption; desorption; selective recognition

1. Introduction

Cobalt(II) is an essential element not only for life in mammals but also for plants and lower forms of organisms. Commonly, cobalt(II) ions (Co^{2+}) are introduced into food chains through soil, water and air. However, the ingestion or inhalation of large dose of this kind of heavy metal ion may lead to toxic effects [1]. Thus the determination trace and ultra trace amount of Co^{2+} is very important in the context of environmental protection, food safety as well as agricultural chemistry. Due to their usually low concentrations and matrix interferences, the direct determination of Co^{2+} in environmental samples is limited [2]. In previous work, exclusive cation exchange resins [3], solid phase extraction (SPE) [4,5], liquid membrane [6–8], coprecipitation [9] and liquid–liquid

---

*Corresponding author. Email: yys@ujs.edu.cn

ISSN 0306–7319 print/ISSN 1029–0397 online

DOI: 10.1080/03067310903502752
http://www.informaworld.com

extraction system [10] were applied to selective separation and enrichment Co^{2+} from environmental samples, among which SPE was proved to be an efficient and low cost alternative. High priority has then been given to the development of new sorbents or extractants and to increase their selectivity, adsorption capacity and regeneration characters.

Molecular imprinting is a convenient and powerful technique for synthesising functional polymers that are capable of high molecular recognition. This potential technique consists of polymerising a functional monomer and mixing with a template in the presence of a cross-linking agent. Then removal of the template leaves behind an imprinted cavity in the molecular imprinted polymer (MIP) which provides an artificial receptor-like binding site for this template [11]. Ion imprinted polymer (IIP) is similar to the MIP, but it recognises the target ion after imprinting, while retaining all the virtues of MIP [12]. Rao *et al.* briefly reviewed IIP and its interesting applications in solid phase extraction (SPE) [13]. A particularly promising IIP-SPE application is the preconcentration or the selective separation of trace amounts metal ions from other coexisting complex matrixes including Cu^{2+} [14], Ni^{2+} [11], Hg^{2+} [15], Fe^{3+} [16], Cr^{3+} [17], Cd^{2+} [18], Zn^{2+} [19], Sm^{3+} [20], Th^{4+} [21], and Dy^{3+} [22]. In nearly all of these studies, selective recognition for target template ion over the other coexisting ions was satisfactory.

Takagi's group first proposed surface-imprinting technique in 1992 by which they utilised an amphiphilic functional monomer forming a stationary complex with the template ion at the interface of the emulsion. After polymerisation and removing the template ion, IIP carring the functional groups spatially on their surface and giving recognition sites with preferential rebinding ability for the template ion was obtained [23]. Subsequently, various surface-imprinting systems offering faster mass transfer kinetics were established. Yilmaz *et al.* [24] applied a surface imprinting technique combined with chitosan (CTS) incorporated sol-gel process to synthesise a novel IIP possessing macroporous surface and functional ligand. He *et al.* [25] synthesised a new ion-imprinted thiol-functionalised silica gel sorbent by a surface-imprinting technique in combination with a sol-gel process for selective online SPE of Cd^{2+}. The satisfactory results described that the surface ion-imprinting technique in combination with the sol-gel process was a versatile method to prepare the size, shape, charge selective inorganic materials, and inorganic-organic hybrid materials with specific functions and affinity.

As a hydrated octahedral layered magnesium aluminum silicate mineral, attapulgite has three binding sites, such as O in the Si–O tetrahedron, H_2O connected to Mg and Si–OH from the surface of Si–O tetrahedron. The special binding sites of attapulgite enable it to adsorb cations, anions and a portion of small molecules. CTS has many reactive amino groups and hydroxyl groups, which offers a possibility to form a large variety of useful derivatives which can be made available via graft reactions and ionic interactions [26]. Glycidoxypropyltrimethoxysilane (KH-560) is an epoxy-siloxane with trimethoxy anchor groups. Due to the non-toxicity and biodegradability compared to glutaraldehyde (GA) and ethylene glycol diglycidy1 ether (EGCE), KH-560 is a novel cross-linking agent.

In our work, CTS was chosen as the monomer to complex with Co^{2+}, and KH-560 was used to functionalise the support material (i.e. attapulgite). Then a new surface-coated ion imprinted polymer, Co-IIP, was synthesised using a surface imprinting technique combined with a CTS incorporated sol-gel process. The preparation method, main characteristic features and application of Co-IIP to selective adsorption Co^{2+} from aqueous solution are described and discussed in detail in this paper.

2. Experimental

2.1 *Instruments and apparatus*

Infrared spectra ($4000 \sim 400\,\mathrm{cm}^{-1}$) were recorded on a Nicolet NEXUS 470 FT-IR apparatus (USA). Microwave Digestion System (MDS-2003F model) was purchased from Sineo Microwave Chemistry Technology (Shanghai, China). Scanning electron microscopy (SEM) images were obtained at 15.0 kV on a Hitachi S-4800 (Hitachi, Japan) field emission scanning electron microscope. A Varian Liberty 150 AX Turbo model inductively coupled plasma-atomic emission spectroscopy (ICP-AES) was used for the determination of the Co^{2+} concentration. The main operating conditions of ICP-AES were the instrumental parameters as follows: 1.0 kw (power), $15.0\,\mathrm{L\,min}^{-1}$ (plasm flux rate), $1.5\,\mathrm{L\,min}^{-1}$ (accessorial gas flux rate), 200 kPa (atomised gas), 15 rpm (pump speed), 10 s (cleanout time), 15 s (stabilisation time).

2.2 *Reagents and materials*

A stock Co^{2+} solution ($1.0\,\mathrm{g\,L}^{-1}$) was prepared by dissolving $Co(NO_3)_2 \cdot 6H_2O$ (Sinopharm Chemical Reagent Co., Shanghai, China) and diluting with doubly deionised water (DDW). The standard solutions and testing solutions were prepared by appropriated dilution with DDW from the stock solution respectively. Chitosan (CTS) with 98% deacetylation and an average molecular weight of $6 \times 10^4\,\mathrm{g\,mol}^{-1}$ (Yuhuan Biomedical Corp., China) was used as functional monomer. ϒ-glycidoxypropyltrimethoxysilane (KH-560) was functioned as a cross-linking agent (Nanjing Shuguang Chemical Group Co., China). Attapulgite, with average size of 92 nm, was supplied by the Nanjing Yadong Aotu Mining Inc. in China. Prior to use, attapulgite was activated by dispersing in $0.1\,\mathrm{mol\,L}^{-1}$ NH_4Cl 10 h at room temperature. All the other chemicals used were analytical grade, and DDW was used throughout this work.

2.3 *Preparation and characterisation of Co-IIP*

An amount of 3.0 g CTS as functional monomer and 0.2 g $Co(NO_3)_2 \cdot 6H_2O$ as template ion were dissolved in 80 mL of $0.1\,\mathrm{mol\,L}^{-1}$ HAc aqueous solution. After stirring for 1.0 h, 15 mL of KH-560 as a cross-linking agent was added into the mixture. Then, the reaction was initiated at 25°C and maintained for 3.0 h with continuous stirring at 300 rpm. After that, the product was treated in an ultrasonic bath for 20 min to be dispersed equably, and then a portion of activated attapulgite was added under the condition of stirring. The wet bead was allowed to evaporate at room temperature to complete the cross-linking reaction and gelation. The dry product was ground and washed with $1.0\,\mathrm{mol\,L}^{-1}$ H_2SO_4 to completely leach the coordinated Co^{2+}, and then washed several times with DDW and $0.1\,\mathrm{mol\,L}^{-1}$ $NH_3 \cdot H_2O$ to ensure the neutralisation of hydrogen ions. Then the polymer was filtered, dried at 50°C under vacuum, ground and sifted with 100 meshes, resulting in the desired Co(II)-imprinted polymer with attapulgite as a support material (Co-IIP). By comparison, the non-imprinted polymer (NIP) was also prepared as a blank in parallel but without the addition of $Co(NO_3)_2 \cdot 6H_2O$.

In order to gain the structural characteristics and imprinting mechanism of Co-IIP, the characterisation of attapulgite, Co-IIP and NIP were investigated by FT-IR and SEM.

2.4 *Adsorption experiments*

Adsorption of Co^{2+} on sorbents (i.e. attapulgite, Co-IIP and NIP) from aqueous solutions was studied in batches. Effects of the pH value of the medium and weight of sorbents on the adsorption rate and adsorption capacity were studied. For this purpose, 50 mL volumes of aqueous solutions containing different amounts of Co^{2+} (in the range of $3.0 \sim 400\,\mathrm{mg\,L^{-1}}$) were treated with different weight of sorbent at room temperature and magnetically stirred at a speed of 400 rpm for 15 min. Different pH values were adjusted with diluted HCl and $NH_3 \cdot H_2O$. After the desired 90 min, the concentration of the Co^{2+} in the aqueous phase was measured by using the ICP-AES. The experiments were performed in replicates of three, and the samples were also analysed in replicates of three. Finally the percentage adsorption (E%) and capacity ($Q\,\mathrm{mg\,g^{-1}}$) were calculated using the Equations (1) and (2).

$$E = [(C_0 - C_e)/C_0] \times 100\%, \tag{1}$$

$$Q = [(C_0 - C_e)V]/W. \tag{2}$$

C_0 ($\mathrm{mg\,L^{-1}}$) and C_e ($\mathrm{mg\,L^{-1}}$) are the initial and equilibrated concentration of Co^{2+}, respectively. V (mL) and W (g) are the solution volume and the mass of sorbent, respectively.

2.5 *Selective recognition experiments*

To measure the selective recognition of Co-IIP, the competitive metal ions recognition studies were performed. Compared with Co^{2+}, Ba^{2+}, Pb^{2+}, Ni^{2+}, Cd^{2+} and Cu^{2+} all have the same charge and especially Ni^{2+}, Cu^{2+}, Fe^{3+} have similar ionic radii, so they were chosen as the competitive metal ions. During the experiment, the coexisting ions (i.e., $Co^{2+}, Ba^{2+}, Pb^{2+}, Ni^{2+}, Cd^{2+}, Fe^{3+}$ and Cu^{2+}) solution which every kind ion contained 150 μg was transferred to a 50 mL flask. Under the optimal conditions, certain amount of sorbents (i.e, attapulgite, Co-IIP or NIP) was added. After adsorption equilibrium, the concentration of the unadsorbed ions in the liquid phase was determined directly by ICP-AES. The distribution and selectivity coefficients of Ba^{2+}, Pb^{2+}, Ni^{2+}, Cd^{2+}, $Fe^{3+}$and Cu^{2+} with respect to Co^{2+} can be obtained from equilibrium binding data according to Equations (3) and (4).

$$K_d = [(C_i - C_f)/C_f](V/W). \tag{3}$$

In Equation (3), K_d represents the distribution coefficient; C_i ($\mathrm{mg\,L^{-1}}$) and C_f ($\mathrm{mg\,L^{-1}}$) represent the initial and final concentration of metal ion in solution, respectively; V is the volume of the coexisting ions solution (mL); W is the weight of sorbent used (g). The selectivity coefficient (k) for the binding of a specific metal ion in the presence of competitor species can be obtained according to the following equation:

$$k = K_{d[Co]}/K_{d[M]}. \tag{4}$$

$K_{d[Co]}$ and $K_{d[M]}$ represent the distribution coefficients of Co^{2+} and competitive metal ions, respectively. A comparison of the k values of the Co-IIP with the competitive metal ions allows an estimation of the effect of imprinting on selective recognition. A relative selectivity coefficient k' can be defined as in Equation (5). The selectivity coefficients of Co-IIP and NIP are k_{i} and K_{n}, respectively.

$$k' = k_{\mathrm{i}}/k_{\mathrm{n}}. \tag{5}$$

2.6 *Desorption and regenerative capacity*

Desorption of Co^{2+} ions was studied with desorption agents: H_2SO_4 solutions (4.0 mol L^{-1}). The saturated Co-IIP was placed in a desorption medium and stirred continuously (at a stirring rate of 300 rpm) for 30 min at room temperature. The desorption ratio was calculated from the final Co^{2+} concentration in the desorption medium. In order to test the regenerative capacity of the Co-IIP beads, the Co^{2+} adsorption-desorption procedure was repeated four times by using the same condition.

2.7 *Sample preparation*

The river sediments were collected from the Yudai River and Yangtse River, Zhenjiang, China. Each 0.2 g sediment sample was digested by microwave in the presence of 1.0 mL H_2O_2, 2.0 mL HF and 5.0 mL aqua regia. The digested samples were immediately filtered through a millipore cellulose nitrate membrane (pore size was 0.45 mm). Then filtrates were diluted to 100 mL and stored in polyethylene bottles.

3. Results and discussion

3.1 *Characteristics of Co-IIP, NIP and attapulgite*

3.1.1 *FT-IR results*

FT-IR spectra of raw materials and prepared polymers are shown in Figure 1. A strong and multi-overlapped peak around 3452 cm^{-1}, from stretching vibrations of N–H and O–H in CTS (Figure 1b), shifted to the 3415 cm^{-1} and obviously became narrow in Co-IIP before leaching the Co^{2+} (Figure 1d). Compared with CTS, the characteristic feature of

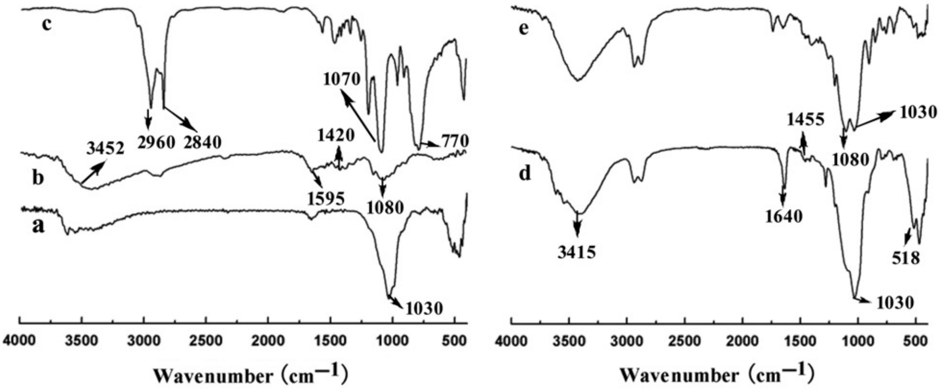

Figure 1. FT-IR spectras of attapulgite (a), CTS (b), KH-560 (c), Co-IIP before (d) and after leaching the Co^{2+} (e).

δ_sN–H at 1595 cm^{-1} and ν_{as}C–N at 1420 cm^{-1} increased to 1640 cm^{-1} and 1455 cm^{-1} in Figure 1d, respectively. Moreover, the absorption peak of C–OH at 1080 cm^{-1} was inconspicuous in Figure 1d in which a new peak at 518 cm^{-1} also assigned to the Co(II)–O appeared. All the facts from the observed excursion of peaks suggested that during the process of mixing CTS and Co^{2+}, Co^{2+} coordinated to –OH and –NH$_2$ simultaneously in CTS and formed the complex Co(II)–CTS resulting in CTS array around the template Co^{2+} with a specific geometry. As shown the FT-IR spectra of Co-IIP (Figure 1e), after leaching the coordinated Co^{2+}, the absorption peak at 518 cm^{-1} which assigned to the Co(II)–O disappeared and the characteristic feature of C–OH at 1080 cm^{-1} was formed. These facts verified the conclusions mentioned above.

The characteristic feature of KH-560 is mentioned in Li *et al.*'s work [27] and compared with KH-560, the peak intensity of –CH$_3$ significantly decreased and the characteristic feature of epoxy group vanished in Co-IIP before adding attapulgite. Moreover, typical Si–O–Si band around 1090 cm^{-1} was present as well. These results confirmed that KH-560 successfully connected with complex from CTS–Co(II) going with ring-opening process, resulting in the desired Si–O–Si network with high degree of cross-linkage. Then, the self-condensation and co-condensation between silanols from self-hydrolysis of siloxane and attapulgite surface took place simultaneously [28]. Eventally, the overlapped absorption band of Si–O–Si from cross-linking reaction and condensation was obtained in Figure 1d.

3.2 *Morphological structure*

The Co-IIP was characterised using scanning electron microscopy (SEM) in order to discover its surface morphological images. SEM image of Co-IIP before leaching the Co^{2+} was obtained in order to know the effect of removal of Co^{2+} from the polymer. Then the SEM images were depicted as Figure 2a and b for Co-IIP before and after leaching the Co^{2+}, respectively. Compared with the attapulgite which was mentioned in Li *et al.*'s work [27], the surface of Co-IIP before leaching the Co^{2+} and Co-IIP were both ruleless and agglomerate due to coating with the products of the cross-linking and imprinting reaction. Also, it is clear that Co-IIP displayed a slightly rough surface with many cavities and the pore size was in the nano-range, corresponding to the ion size. Moreover, without the

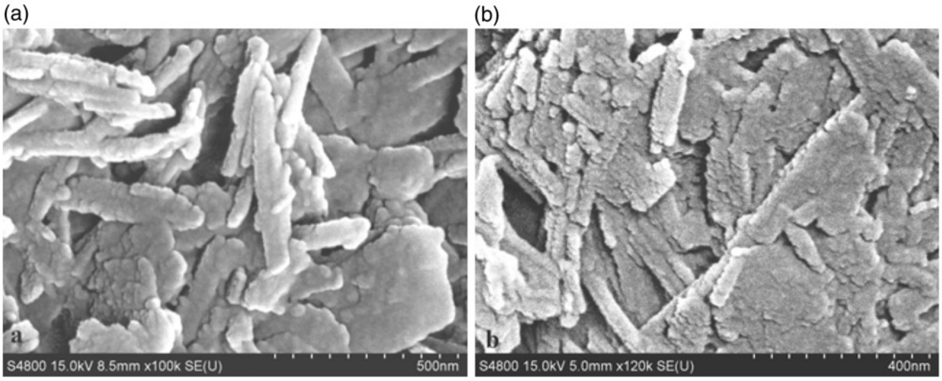

Figure 2. SEM micrographs of Co-IIP before (a) and after (b) leaching the Co^{2+}.

process of leaching template ions, Co-IIP before leaching the Co^{2+} exhibited a slippery surface with a claval shape which was the same as attapulgite. By coordinating between Co^{2+} and –OH in CTS, –OH was shielded in the cross-linking process, so it overcame the decrease in adsorption capacity caused by the loss of binding sites [28].

3.3 *The imprinting mechanism for Co-IIP*

Based on the analysis of structure and characters above, the imprinting mechanism for Co-IIP was discussed in detail. The proposed imprinting mechanism for Co-IIP mainly contained four steps which were shown in Figure 3 [27]. First, template Co^{2+} coordinated to the –OH and $–NH_2$ from functional monomer CTS, and the complex from CTS–Co^{2+} was obtained (Figure 3a). In the second part, CTS–Co^{2+} and KH-560 attended polymeric reaction, then the cross-linked polymer network was formed (Figure 3b). Meanwhile, silanol groups were generated through acid-catalysed self-hydrolysis of KH-560. The next step is the self-condensation and co-condensation of –OH between silanols from siloxane and attapulgite surface, then the product was coated onto the surface of attapulgite (Figure 3c). Then, Co^{2+} was leached from the surface of Co-IIP, leaving behind its impression in the form of a cavity with appropriately oriented function (Figure 3d).

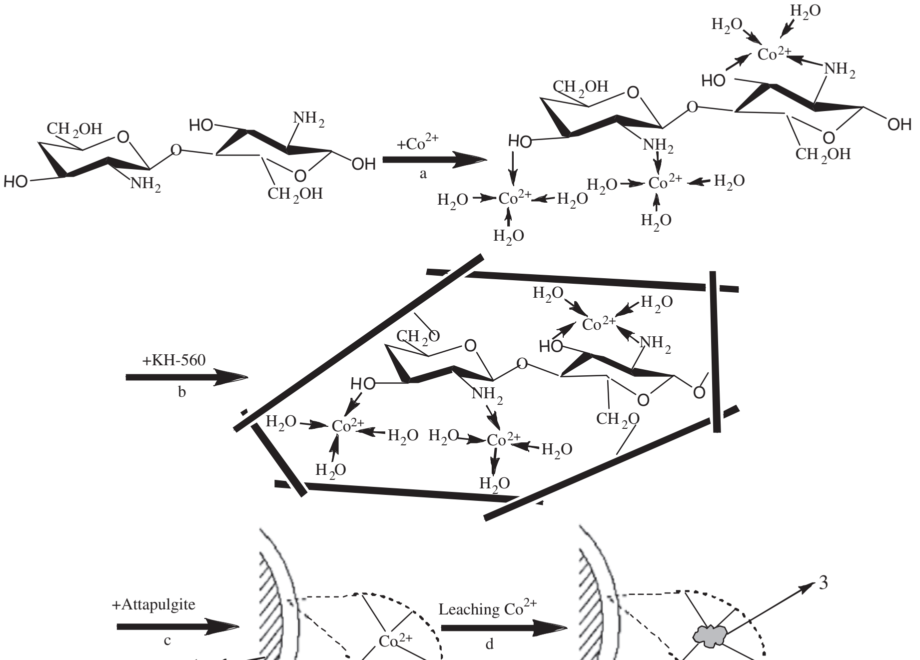

Figure 3. Proposed scheme of imprinting mechanism for Co^{2+}-IIP. 1: attapulgite; 2: coating-layer; 3: binding site.

4. Adsorption of Co^{2+} from aqueous solutions

4.1 *Adsorption optimisation of Co^{2+} in the batch method*

During the batch experiments, a set of solutions (50 mL volume each) was prepared, containing 150 mg of Co^{2+}. The pH value of these solutions were adjusted between $3.0 \sim 7.0$, and the weight of sorbents were used from $0.1 \sim 0.25$ g, then the recommended procedure was applied. The experimental parameters (i.e. pH value, weight of sorbents) were varied and the percentage adsorption of Co^{2+} was calculated from the ICP-AES. The corresponding results were listed in Table 1. It can be noticed from the results that when the pH value of medium was at 4.0, mass of Co-IIP was 0.25 g and enrichment time was 90 min, the percentage adsorption of Co^{2+} reached 100%. On the other hand, without special size of the cavities and the specific binding sites with functional groups in a predetermined orientation, NIP has lowest percentage adsorption of Co^{2+} which was only 28.33% even if under its optimal adsorption conditions. Moreover, the adsorption capacity for Co^{2+} followed the order Co-IIP > attapulgite > NIP. Then the Co-IIP and attapulgite were chosen as sorbents to carry out residual experiments.

4.2 *Adsorption kinetics*

The effect of adsorption time on the attapulgite and Co-IIP adsorption Co^{2+} from solutions at optimal condition and at 25 °C is given in Figure 4. The adsorption kinetics of Co-IIP is faster than that of attapulgite due to the imprinting effect. The adsorption rate increased with time and revealed a rapid value during the first 40 min of enrichment, after which the adsorption rate increased slowly. The rapid step is probably due to the abundant binding sites on the sorbents and with the gradual decrease of binding sites slowing down the ions adsorption action from bulk solution. Finally, the equilibrium conditions for attapulgite and Co-IIP were obtained. Furthermore, owing to the special binding sites which were tailored to Co(II) in shape, size and coordination, the percentage adsorption of Co^{2+} onto Co-IIP attained after equilibrium was 100% which was much higher than that of attapulgite (90.6%).

Table 1. Effects of pH value and doage of sorbents on the adsorption Co^{2+}.

	Adsorption ratio (%)		
Parameters	Attapulgite	NIP	Co-IIP
pH value (Weight of each sorbent was 0.2 g)			
3.0	86.13 ± 0.03	7.33 ± 0.20	86.33 ± 0.02
4.0	90.17 ± 0.04	12.67 ± 0.30	99.33* ± 0.05
5.0	90.60* ± 0.03	25.33* ± 0.10	98.67 ± 0.03
6.0	90.07 ± 0.02	24.67 ± 0.20	97.33 ± 0.03
7.0	89.90 ± 0.05	23.67 ± 0.20	95.00 ± 0.01
Weight of sorbent (g) (pH value for attapulgite, NIP, Co-IIP was 5.0, 5.0, 4.0, respectively)			
0.1	86.97 ± 0.04	9.67 ± 0.30	94.33 ± 0.03
0.15	89.30 ± 0.01	14.33 ± 0.20	97.33 ± 0.05
0.2	90.60 ± 0.03	25.33 ± 0.10	99.33 ± 0.02
0.25	91.93* ± 0.03	28.33* ± 0.30	100.00* ± 0.01

Note: The value following '*' represents the optimum conditions for the adsorption of Co^{2+}.

In order to examine the controlling mechanism of adsorption process such as mass transfer and chemical reaction, the kinetic data obtained from the effect of adsorption time on the attapulgite and Co-IIP have been analysed using a pseudo-second-order rate equation. It was described in Equation (6):

$$t/q_t = 1/k_2 q_e^2 + t/q_e, \tag{6}$$

where q_e and q_t are the amount of Co^{2+} adsorbed (mg g^{-1}) onto the sorbent at the equilibrium and at time t (min), respectively. Value of k_2 (g mg^{-1} min^{-1}) were calculated from plotting t/q_t versus t.

The data fitted the Equation (6), and the adsorption kinetic constants and linear regression values with standard deviation were summarised in Table 2. The data exhibited a linear relationship for Co-IIP and attapulgite with R^2 above 0.999. The calculating equilibrium adsorption capacity ($q_{e,c}$) from the pseudo-second-order model (0.676 mg g^{-1} and 0.635 mg g^{-1}) were close to the experimental adsorption capacity (q_e) (0.6 mg g^{-1} and 0.544 mg g^{-1}) for Co-IIP and attapulgite. The results showed that this model can be

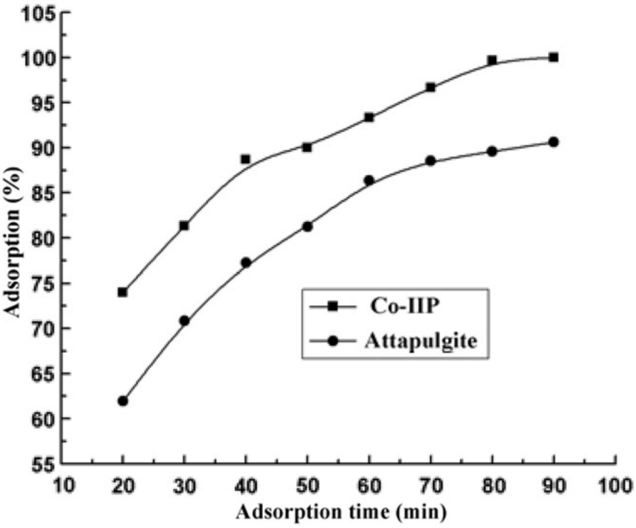

Figure 4. The effect of adsorption time on the adsorption Co^{2+}.

Table 2. Kinetic parameters of the pseudo-order-rate equation for Co^{2+} adsorption onto Co-IIP and attapulgite.

Kinetic parameters	Co-IIP	Attapulgite
k_2 (g mg^{-1} min^{-1})	0.1368	0.1089
q_e (mg g^{-1})	0.6	0.544
$q_{e,c}$ (mg g^{-1})	0.676	0.635
R^2	0.9996	0.9997
SD	1.1072	1.0615
X^2	<0.0001	<0.0001

applied to predict the adsorption kinetic and the overall rate-constant appeared to be controlled by a chenmisorption mechanism through sharing or exchange of electrons between the sorbent surface and Co^{2+} [14]; k_2 value is an indicator to express the adsorption velocity. As shown in Table 2, the constant was greater for Co-IIP than that of attapulgite. Therefore, the kinetics for the adsorption of Co^{2+} also followed the order Co-IIP>attapulgite.

4.3 *Adsorption isotherms*

The adsorption isotherms for attapulgite, A-IIP and S-IIP were shown in Figure 5. When the equilibrium concentration increased, the adsorption capacity of Co-IIP first increased sharply, then increased slightly, and finally reached to the maximum point. The adsorption isotherms of attapulgite and A-IIP were similar in shape, and the adsorption capacity increased slowly during the whole process. The equilibrium data were then fitted to the Langmuir adsorption isotherm assuming monolayer adsorption onto a surface with a finite number of identical sites and was expressed as follows [29]:

$$C_e/Q_e = 1/(Q_m K_L) + C_e/Q_m, \tag{7}$$

where C_e is the equilibrium concentration of Co^{2+} in solution ($mg\,L^{-1}$), Q_e is the adsorption capacity at equilibrium ($mg\,g^{-1}$), Q_m is the maximum adorption capacity of the *sorbent*, and K_L represents the affinity constant.

The Langmuir adsorption isotherm constants for attapulgite, NIP and Co-IIP were listed in Table 3. The experimental values of Q_m ($Q_{m,e}$) 20.5 and 31.5 $mg\,g^{-1}$ were very close to the calculated values (i.e. 26.86 and 32.05 $mg\,g^{-1}$), respectively. The value of K_L for Co-IIP (0.01118 $L\,mg^{-1}$) indicated that it has obvious superiority to adsorb Co^{2+} than attapulgite (0.01020 $L\,mg^{-1}$) by imprinting effect. Moreover, high correlation coefficients r^2 value (i.e. 0.99839 and 0.99207) suggested that the Langmuir equation gave a good linear fit to the adsorption isotherm.

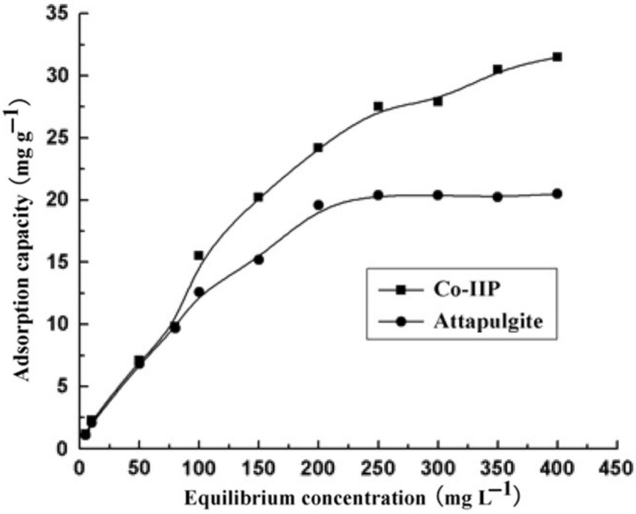

Figure 5. Adsorption isotherms for Co-IIP and attapulgite.

For predicting the favourability of an adsorption system, the Langmuir equation can also be expressed in terms of a dimensionless separation factor R_L defined as follows [30]:

$$R_L = 1/(1 + C_0 K_L). \tag{8}$$

C_0 is the initial concentration of Co^{2+}. The R_L indicates the favourability and the capacity of the adsorbent/adsorbate system. When $0 < R_L < 1$, it represents good adsorption. Table 4 showed the data of R_L for adsorption Co^{2+}. According to the results, it was known that the present adsorption systems were favourable for attapulgite and Co-IIP, and the adsorption Co^{2+} was more favourable at higher initial Co^{2+} concentrations than at lower ones.

4.4 *Selective recognition of Co^{2+} from aqueous solutions*

The K_d, k and k' of attapulgite, NIP and Co-IIP for Co^{2+} were summarised in Table 5. Due to the imprinting effect, along with the increase of surface area and binding sites for

Table 3. Langmuir adsorption isotherm constants for attapulgite and Co-IIP adsorption Co^{2+}.

Sorbents	Q_m (mg g^{-1})	$Q_{m,e}$ (mg g^{-1})	K_L (L mg^{-1})	r^2	SD
Attapulgite	26.86	20.5	0.0102	0.9921	0.6551
Co-IIP	32.05	31.5	0.0112	0.9984	0.1791

Table 4. Separation factor R_L for attapulgite, NIP and Co-IIP adsorption Co^{2+}.

C_0 (mg L^{-1})		5	10	50	80	100	150	200	250	300	350	400
R_L	Attapulgite	0.9515	0.9074	0.6623	0.5507	0.4951	0.3953	0.3290	0.2817	0.2463	0.2188	0.1969
	Co-IIP	0.9471	0.8994	0.6414	0.5279	0.4721	0.3736	0.3090	0.2635	0.2297	0.2035	0.1827

Table 5. Selective recognition of the attapulgite, NIP and Co-IIP for Co^{2+}.

Metal ions	Co-IIP		Attapulgite		NIP		
	K_d (mL g^{-1})	k	K_d (mL g^{-1})	k	K_d (mL g^{-1})	k	k'
Co^{2+}	190.80	–	63.33	–	23.19	–	–
Pb^{2+}	170.25	1.12	124.97	0.52	51.43	0.45	2.49
Ba^{2+}	23.79	8.02	8.27	7.90	13.91	1.67	4.81
Ni^{2+}	29.72	6.42	53.91	1.21	21.51	1.08	5.96
Cd^{2+}	78.43	2.43	30.39	2.15	32.11	0.72	3.37
Cu^{2+}	45.33	4.21	66.59	0.98	27.27	0.85	4.95
Fe^{3+}	52.43	3.64	75.04	0.87	30.54	0.76	4.79

Co-IIP, K_d and k value of Co-IIP showed a significant increase than the values of NIP. Because attapulgite has three special binding sites which were mentioned above, it has good adsorption for many metal ions, and there was no exception for Co^{2+}. But without the specific binding sites with functional groups in a predetermined orientation and special size of the cavities, K_d and k values of attapulgite have obvious differences with Co-IIP. It is the case that k' is an indicator to express adsorption affinity of recognition sites to the template Co^{2+}. The k' results showed that the selective recognition for the Co-IIP were nearly 6.0 ~ 14.0 times greater than that of the NIP. These findings indicated that the selective recognition of Co-IIP for Co^{2+} was significantly higher than NIP and attapulgite.

The competitive adsorption of metallic ions on the Co-IIP and NIP were investigated by the batch procedure. The results showed that NIP has a low adsorption around 20% for each competitive metallic ions. Although some ions have similar radii with Co^{2+}, and some ions also have high affinity with the $-NH_2$ or –OH, the Co(II)-IIP still exhibited high selectivity for extraction of Co^{2+} in the presence of other metal ions. So it demonstrated that the approvingly selective recognition of Co-IIP was governed by the ionic radius of original template ion, affinity between the host matrix and the guest substance [31].

4.5 *Enrichment factor and regenerative capacity*

The enrichment factor is an important parameter for evaluating a sorbent, so it was studied by recommended desorption procedure by changing volume of sample solution and keeping the total amount of adsorbed Co^{2+} onto Co-IIP to 150 µg. In this case, 10, 25, 50, 100, 150 and 200 mL of Co^{2+} solutions were used in the adsorption-desorption procedure. When the Co(II) sample volume was up to 100 mL, the recovery of Co^{2+} could be up to 95%. It may be due to the strong competitive adsorption of the hydrogen ion, demonstrating that the protonation of –OH and $-NH_2$ could prevent the adsorption for Co^{2+}. Then, 100 mL of sample solution was chosen for the enrichment of Co^{2+} from the sample solution. An enrichment factor of 10 was obtained because 10 mL of desorption agent was used.

In order to obtain the regenerative capacity of Co-IIP, adsorption-desorption cycles were carried out four times by using the same sorbent in a batch experiments. The results showed that after the four cycles regeneration, the adsorption capacity of Co-IIP for Co^{2+} was about 13.42% loss in pure Co^{2+} solution, and about 16.17% loss in the coexisting ions solution. The results illustrated that Co-IIP has good regenerative capacity, even in a competing metallic ions environment.

4.6 *Effect of interference*

In order to study of interference by foreign ions, such as K(I), Na(I), Ca(II), Mg(II), Fe(III), Zn(II), Mn(II), Cu(II), Cd(II), Cl(I), Si(IV) and W(VI), a 50 ml of sample solutions, containing 150 µg of Co(II) and one foreign ion with varying amount, was taken and operated according to the proposed adsorption experiment procedure. The tolerance limit of the each foreign ion, defined as the largest amount making the recovery of Co(II) less than 90%, the results were investigated and are given in Table 6. It showed that the effects of foreign ions at given amount were negligible. The possible factor was that Co-IIP has the specific binding sites with functional groups in a predetermined orientation and special size of the cavities. It implied that Co-IIP had a promising application in determination of a real environmental sample which contained diverse ions.

4.7 *Analytical precision and the detection limit*

Under the optimal conditions, 13 portions of standard solutions were enriched and analysed simultaneously following the general procedure. The relative standard deviation (RSD) of the method was lower than 1.35%, which indicated that the method had good precision for the analysis of trace Co(II) in solution samples. According to the definition from IUPAC [32], the detection limit of the method was calculated based on three times of the standard deviation of 13 runs of the blank solution. The detection limit (3σ) of the proposed method was $0.0263\,\mathrm{mg\,L^{-1}}$. The calibration curve was linear within concentration range from 0.5 to $8.0\,\mathrm{mg\,L^{-1}}$. Calibration graphs obeyed the equation $A = 0.0937C$ ($\mathrm{mg\ L^{-1}}$) $+0.0106$ ($r^2 = 0.99987$). (A is the absorbance, C is concentration of Co^{2+} in solution and r^2 is correlation coefficient.)

4.8 *Recovery rate for river sediment samples*

The prepared Co-IIP was applied for selective separation and determination of trace Co^{2+} in two river sediment samples with the standard addition method. The results listed in Table 7 showed that the recoveries were reasonable for trace analysis in range of

Table 6. Effect of interference on the recovery of Co^{2+}.

Interference	Added (μg)	Recovery (%)	Interference	Added (μg)	Recovery (%)
K^+	4000	96.50	Cu^{2+}	1000	94.32
Na^+	3000	95.12	Mn^{2+}	800	93.71
Ca^{2+}	2000	94.17	Cd^{2+}	800	95.62
Mg^{2+}	2000	92.32	Cl^-	7000	97.33
Fe^{3+}	1000	92.74	SiO_3^{2-}	700	90.25
Zn^{2+}	1000	93.68	WO_4^{2-}	1000	91.49

Table 7. Analytical results for the determination trace Co^{2+} in river sediment samples ($n = 3$).

River sediment sample	Co^{2+} added ($\mathrm{mg\,L^{-1}}$)	Concentration of Co^{2+} ($\mathrm{mg\,L^{-1}}$)		Recovery (%)
		Found	Sum	
Yudai River	0.50	0.632 ± 0.004	1.102 ± 0.004	97.3
	1.00		1.601 ± 0.003	98.1
	2.00		2.604 ± 0.001	98.9
	3.00		3.635 ± 0.005	100.8
Yangtse River	0.50	0.217 ± 0.006	0.682 ± 0.002	95.1
	1.00		1.195 ± 0.001	98.2
	2.00		2.201 ± 0.003	99.3
	3.00		3.225 ± 0.005	100.2

95.1 ~ 100.8%. Evidently, the method is feasible and provides satisfactory results. The results indicated the suitability of Co-IIP for selective solid-phase extraction and determination of trace Co^{2+} in environmental samples.

5. Conclusions

A new type of Co(II) ion imprinted polymer was successfully prepared by the surface molecular imprinting concept combined with sol-gel process. In steps, Co(II) ion imprinted composite material coating on the surface of attapulgite was carried out using Co^{2+} as a template, CTS as a functional monomer and KH-560 as a cross-linker. Thus prepared Co-IIP exhibited several special characteristics, such as mild imprinting reactive conditions, fine configuration, fast adsorption-desorption procedure, proper static adsorption capacity, satisfactory recognition, and obvious regenerative capacity for Co^{2+}. The method was successfully applied to the selective solid-phase extraction of trace Co^{2+} in river sample sediment sample solutions. The precision and accuracy of the method are satisfactory.

Acknowledgements

This work was financially supported by the National Natural Science Foundation of China (No. 20877036).

References

[1] G. RaúlA, G. JoséA, O. Roberto, D.M. Luis, and C. Soledad, Talanta **76**, 669 (2008).
[2] M. Tuzen, K.O. Saygi, and M. Soylak, J. Hazard. Mater. **152**, 632 (2008).
[3] L. Barron, M.Ó. Toole, D. Diamond, P.N. Nesterenko, and B. Paull, J. Chromatogr. A **1213**, 31 (2008).
[4] P.H. Pacheco, P. Smichowski, G. Polla, and L.D. Martinez, Talanta **79**, 249 (2009).
[5] A. Nilchi, H. Atashi, A.H. Javid, and R. Saberi, Appl. Radiat. Isot. **65**, 482 (2007).
[6] R.A. Kumbasar, J. Membr. Sci. **338**, 182 (2009).
[7] P.K. Parhi and K. Sarangi, Sep. Purif. Technol. **59**, 169 (2008).
[8] M.S. Gasser, N.E. El-Hefny, and J.A. Daoud, J. Hazard. Mater. **151**, 610 (2008).
[9] M. Soylak and H. Balgunes, J. Hazard. Mater. **155**, 595 (2008).
[10] J. Wang, W. Yang, J. Ren, M. Guo, X.D. Chen, W.B. Wang, and J.Z. Gao, Chin. Chem. Lett **19**, 1103 (2008).
[11] Q. Li, H.J. Su, and T.W. Tan, Biochem. Eng. J. **38**, 212 (2008).
[12] N. Masque, R.M. Marce, and F. Borrull, Trends Anal. Chem. **20**, 477 (2001).
[13] T.P. Rao, R. Kala, and S. Daniel, Anal. Chim. Acta **578**, 105 (2006).
[14] Y.M. Ren, M.L Zhang, and D. Zhao, Desalination **228**, 135 (2008).
[15] G.H. Wu, Z.Q. Wang, J. Wang, and C.Y. He, Anal. Chim. Acta **582**, 304 (2007).
[16] X.J. Chang, N. Jiang, H. Zheng, Q. He, Z. Hu, Y.H. Zhai, and Y.M. Cui, Talanta **71**, 38 (2007).
[17] E. Birlik, A. Ersöz, E. Açıkkalp, A. Denizli, and R. Say, J. Hazard. Mater. **140**, 110 (2007).
[18] N. Candan, N. Tüzmen, M. Andac, C.A. Andac, R. Say, and A. Denizli, Mater. Sci. Eng. C **29**, 144 (2009).
[19] J.C. Zhao, B. Han, Y.F. Zhang, and D.D. Wang, Anal. Chim. Acta **603**, 87 (2007).
[20] S. Shirvani-Arani, S.J. Ahmadi, A. Bahrami-Samani, and M. Ghannadi-Maragheh, Anal. Chim. Acta **62**, 82 (2008).

[21] Q. He, X.J. Chang, Q. Wu, X.P. Huang, Z. Hu, and Y.Z. Zhai, Anal. Chim. Acta **605**, 192 (2007).

[22] N. Zhang, B. Hu, and C.Z. Huang, Anal. Chim. Acta **597**, 12 (2007).

[23] K. Tsukagoshi, K.Y. Yu, M. Maeda, and M. Takagi, Bull. Chem. Soc. Jpn. 66, 114 (1993).

[24] E. Yilmaz, O. Ramström, P. Möller, D. Sanchez, and K. Mosbach, J. Mater. Chem. **12**, 1577 (2002).

[25] C.Y. He, Y.Y. Long, J.L. Pan, K. Li, and F. Liu, Talanta **74**, 1126 (2008).

[26] P.K. Dutta, J. Dutta, M.C. Chattopadhyaya, and V.S. Tripathi, J. Polym. Mater. **21**, 321 (2004).

[27] C.X. Li, J.M. Pan, J. Gao, Y.S. Yan, and G.Q. Zhao, Chin. Chem. Lett. **20**, 985 (2009).

[28] F. Li, H.Q. Jiang, and S.S. Zhang, Talanta **71**, 1487 (2007).

[29] A. Benhammou, L. Yaacoubi, B. Nibou, and B. Tanouti, J. Collid Interface Sci. **282**, 320 (2005).

[30] J.H. Huang, Y.F. Liu, Q.Z. Jin, X.G. Wang, and J. Yang, J. Hazard. Mater. **143**, 541 (2007).

[31] O. Vigneau, C. Pinel, and M. Lemaire, Chem. Lett. **2**, 202 (2002).

[32] M. Tuzena, D. Citaka, and M. Soylak, J. Hazard. Mater. **158**, 137 (2008).